

1  
2  
3  
4  
5  
6  
7  
8  
9  
10  
11  
12  
13  
14  
15  
16  
17  
18  
19  
20  
21  
22  
23

---

**Tail-Anchored Inner Membrane Protein ElaB Increases Resistance to Stress  
While Reducing Persistence in *Escherichia coli***

Yunxue Guo<sup>1</sup>, Xiaoxiao Liu<sup>1</sup>, Baiyuan Li<sup>1,2</sup>, Jianyun Yao<sup>1,2</sup>, Thomas K. Wood<sup>3,4</sup>, and Xiaoxue Wang<sup>1\*</sup>

<sup>1</sup>Key Laboratory of Tropical Marine Bio-resources and Ecology, Guangdong Key Laboratory of Marine Materia Medica, RNAM Center for Marine Microbiology, South China Sea Institute of Oceanology Chinese Academy of Sciences, Guangzhou 510301, China, <sup>2</sup>University of Chinese Academy of Sciences, Beijing 100049, China,

<sup>3</sup>Department of Chemical Engineering and the <sup>4</sup>Department of Biochemistry and Molecular Biology, Pennsylvania State University, University Park, PA 16802-4400, USA

\*To whom correspondence should be addressed. Tel: +86 20 89267515; Fax: +86 20 89235490; Email:

xxwang@scsio.ac.cn

**Running title:** ElaB is a stress-related inner membrane protein

**Keywords:** C-tail anchored membrane protein, oxidative stress, heat shock, persistence

24  
25  
26  
27  
28  
29  
30  
31  
32  
33  
34  
35  
36  
37  
38  
39  
40  
41  
42  
43  
44  
45

## ABSTRACT

Host-associated bacteria, such as *Escherichia coli*, often encounter various host-related stresses such as nutritional deprivation, oxidative stress and temperature shifts. There is growing interest in searching for small endogenous proteins that mediate stress responses. Here, we characterized a small C-tail anchored inner membrane protein ElaB in *E. coli*. ElaB belongs to a class of tail-anchored inner membrane proteins with a C-terminal transmembrane domain but lacking an N-terminal signal sequence for membrane targeting. Proteins from this family have been shown to play vital roles such as membrane traffic and apoptosis in eukaryotes; however, their role in prokaryotes is largely unexplored. Here, we found that transcription of *elaB* is induced in the stationary phase in *E. coli*, and stationary-phase sigma factor RpoS regulates *elaB* transcription by binding to the promoter of *elaB*. Moreover, ElaB protects cells against oxidative stress and heat shock stress. However, unlike membrane peptide toxins TisB and GhoT, ElaB does not lead to cell death, and the deletion of *elaB* greatly increases persister cell formation. Therefore, we demonstrate that disruption of C-tail anchored inner membrane proteins can reduce stress resistance; it can also lead to deleterious effects such as increased persistence in *E. coli*.

## IMPORTANCE

*Escherichia coli* synthesize dozens of poorly understood small membrane proteins containing a predicted transmembrane domain. In this study, we characterized the function of the C-tail anchored inner membrane protein ElaB in *E. coli*. ElaB increases resistance to oxidative stress and heat stress, while inactivation of ElaB leads to high persister cell formation. We also demonstrated that transcription of *elaB* is under the direct regulation of stationary phase sigma factor RpoS. Thus, our study reveals that small inner membrane proteins may have important cellular roles during stress response.

46

## INTRODUCTION

47

48

49

50

51

52

Membrane proteins interact with, or are part of, biological membranes, and they separate the cytoplasm from the extracellular environment in all living cells. These membrane proteins are prevalent as they are encoded by 20 to 30% of all genes in most genomes (1, 2). For *Escherichia coli*, the inner membrane is a phospholipid bilayer and integral inner membrane proteins are mostly  $\alpha$ -helical (3). The inner membrane proteins include transporters, channels, receptors, enzymes, and structural membrane-anchoring domains for myriad tasks including energy transduction and cell adhesion (4).

53

54

55

56

57

58

59

60

61

62

63

Most proteins are inserted into the membrane by the well-conserved Sec pathway, consisting of a membrane-spanning translocase SecYEG in bacteria. Many accessory proteins aid in protein targeting and insertion, including the signal recognition particle (SRP) and its cognate membrane receptor FtsY (5). To be tagged to the membrane via the Sec pathway, a protein usually has an N-terminal signal sequence for recognition by the SRP. Translation of the N-terminal signal peptide that target proteins to the SRP pathway is required for directing mRNAs to the membrane (6). In *E. coli*, YidC can be specifically cross-linked to the transmembrane domain of newly synthesized peptides during their membrane insertion via translocons (a complex of proteins associated with the translocation of polypeptides across membranes) (7, 8). Several lines of evidence have revealed that in *E. coli*, as well as in mammalian cells, ribosomes translating inner membrane proteins interact cotranslationally with translocons in the membrane, and this interaction is required for the proper insertion of nascent polypeptides into the membrane (6, 9).

64

65

66

67

68

69

70

71

C- tail anchored inner membrane proteins, a class of proteins characterized by their lack of N-terminal signal sequence, were first identified in eukaryotes, and they play critical roles in membrane traffic, apoptosis and protein translocation in eukaryotes (10-12). Tail-anchored inner membrane proteins have been found in *Streptomyces coelicolor*, and they are capable of targeting proteins to the membrane in the absence of an N-terminal signal sequence; the C-terminal transmembrane domain is sufficient for membrane targeting (13). By considering the distance of the transmembrane domain from the C-terminus (less than 30 residues) and also the lack of an N-terminal signal peptide, 12 proteins were identified as C-terminal anchored proteins in *E. coli* (14). These 12 proteins include those known to be associated with the inner face of the cytoplasmic membrane, such as

72 the flagella assembly protein FIK, the TraL protein involved in F pilus formation and enzymes with hydrophobic  
73 substrates that are expected to be favored by membrane anchorage (15, 16). Only three out of the 12 C-tailed  
74 anchored proteins, YgaM and paralogs ElaB and YqjD, have not been uncharacterized (14). Recently, these three  
75 proteins have been shown to be associated with stationary phase ribosomes (17). Complexes in the inner  
76 membrane of *E. coli* are often involved in key processes such as energy generation, cell division, signal  
77 transduction, and transport (18). Targeting small stress resistance proteins is an emerging area for treating  
78 bacterial infections (19-22); however, there are risks in targeting YgaM, ElaB and YqjD since their function is not  
79 known.

80 In this study, we focus on the physiological role of ElaB when cells encounter external stress. The *elaABCD*  
81 genes in the *E. coli* genome were previously named without a phenotypic explanation. ElaC was renamed as Rbn  
82 and has both endoribonuclease and exoribonuclease activities, while ElaD, previously mis-annotated as a putative  
83 sulfatase/phosphatase, is an efficient and specific de-ubiquitinating enzyme (23-25). It has been reported that ElaB  
84 is mainly expressed in the stationary phase (17), and we demonstrate here that *elaB* transcription is regulated by  
85 the stationary phase sigma factor RpoS. We also provide evidence that ElaB protects cells against heat shock and  
86 oxidative stress. However, unexpectedly, disruption of ElaB greatly increases persister cell formation. Thus, ElaB  
87 represents a new transmembrane protein that participates in various stress responses.

88

89

## EXPERIMENTAL PROCEDURES

90 **Bacterial strains, plasmids, and growth conditions.** The bacterial strains and plasmids used in this study are  
91 listed in **Table 1**. Luria-Bertani (LB) (26) and M9 minimal medium with 0.4% glucose (27) were used as  
92 indicated. The Keio collection (28) and the ASKA library (29) were used for deleting and overexpressing single  
93 genes. Chloramphenicol (30  $\mu\text{g}/\text{mL}$ ) was used for maintaining pCA24N-based plasmids, and kanamycin (50  
94  $\mu\text{g}/\text{mL}$ ) was used for pre-culturing the isogenic knockout mutants.

95 **Construction of plasmids.** For the purification of sigma factor RpoS, the coding region of *rpoS* was amplified  
96 using BW25113 genomic DNA as template with the primer pair listed in **Table S1**. PCR products were purified  
97 using a gel extraction kit (Qiagen, Hilden, Germany), and digested with *Xba*I and *Hind*III and purified with a PCR

98 product purification kit (Qiagen). The purified PCR products were ligated into the pET28b plasmid and  
99 transferred into *E. coli* BL21. The correct construct was verified by DNA sequencing using primer M13.

100 For the promoter activity assay, a 300 nt fragment from -300 to -1 relative to the *elaB* translational start site  
101 was amplified by PCR with primers pHGR01-*PelaB*-f and pHGR01-*PelaB*-r (**Table S1**). The PCR product was  
102 purified and digested with *EcoRI* and *HindIII*, and then was ligated into pHGR01. The correct vector pHGR01-  
103 *PelaB* was verified by DNA sequencing using primer pair pHGR01-f and pHGR01-r listed in **Table S1**. To  
104 perform site mutagenesis of the RpoS binding site in the *elaB* promoter in pHGR01-*PelaB* (pHGR01-M*PelaB*),  
105 from TTCAGG (-35)...TCTATAGTTA (-10) to AAAAAAA (-35)...CCCCCCCCCCC (-10), three rounds of PCR  
106 were performed. The first round PCR was amplified with pHGR01-*PelaB*-f and M-pHGR01-*PelaB*-r2  
107 (**Table S1**) using the wild-type genomic DNA as template, then the purified PCR product was used as template  
108 and the secondary round PCR was amplified with pHGR01-*PelaB*-f and M-pHGR01-*PelaB*-r3 (**Table S1**). The  
109 purified products from the secondary PCR were further used as template and amplified with pHGR01-*PelaB*-f and  
110 pHGR01-*PelaB*-r. The last round PCR products were further cloned into pHGR01 to make pHGR01-M*PelaB*, and  
111 the correct mutation in the *elaB* promoter region in pHGR01-M*PelaB* was validated by DNA sequencing using  
112 primers pHGR01-f and pHGR01-r listed in **Table S1**.

113 **Generation of *mCherry* and *gfp* fused strains.** To generate *elaB::mCherry*, the one step inactivation method (30)  
114 was applied to fuse *mCherry*, which encodes a red fluorescence protein, before the stop codon of *elaB* to generate  
115 protein ElaB-mCherry. The coding region of *mCherry* without its start codon was amplified by PCR using  
116 pmCherry-N1 (Clontech, Mountain View, CA) as template with primers *mCherry*-f and *mCherry*-r. Primer pair  
117 *mCherry*-KM-f and KM-r was used to amplify the kanamycin resistance ( $Km^r$ ) cassette, bordered by FLP  
118 recombination target (FRT) sites, from plasmid pKD4. The PCR products were served as templates in overlapping  
119 extension PCR with primers *mCherry*-f and KM-r to generate a DNA fragment carrying *mCherry* and  $Km^r$   
120 cassettes flanked by about 60 nt regions up- and downstream of *elaB* stop codon. The PCR products were purified  
121 using a gel extraction kit (Qiagen), and purified fragments were electroporated into BW25113/pKD46 competent  
122 cells. Strain of BW25113 *elaB::mCherry* was confirmed by PCR followed by DNA sequencing using primers of

123 conf-f and conf-r. The same procedures were performed to fuse *mCherry* before the stop codon of the *lacZ* gene,  
124 as well as for the construction of the *elaB::gfp* strain.

125 **Protein localization.** For localization of ElaB using the mCherry-ElaB fusion, strains were cultured to a turbidity  
126 at 600 nm of 1.0, washed with 0.85% NaCl, and imaged with fluorescence microscopy (Zeiss Axiophot) using an  
127 oil immersion objective (100×). For localization of ElaB by GFP fusion, overnight cultures of BW25113  
128 harboring pCA24N-*elaB-gfp* or pCA24N-*gfp* were inoculated into LB with chloramphenicol (30 µg/mL) at a  
129 turbidity at 600 nm of 0.1, and 0.5 mM isopropyl-β-d-thiogalactopyranoside (IPTG) was added to induce ElaB-  
130 GFP expression for 2 h before imaged.

131 **Fractionation of membrane proteins.** To study the localization of ElaB, proteins from the inner and outer  
132 membranes were obtained by differential centrifugation as described previously with modification (17, 31). IPTG  
133 (0.5 mM) was added to induce ElaB expression using pCA24N-*elaB* for 3 h. Cell pellets were resuspended in TE  
134 buffer (50 mM Tris-HCl at pH 8.0, 5 mM EDTA), and 1 mg/mL lysozyme (Sigma-Aldrich) was added to lyse the  
135 cells. Cell debris was removed by centrifugation at 3,200 g at 4°C for 10 min. The supernatant was further  
136 centrifuged at 4°C at 500,000 g for 1.5 h, and the pellets (membrane protein fractions) were resuspended in 2 mL  
137 of TE buffer. An aliquot (1/10) of was then loaded on a 20-mL sucrose step gradient prepared with 10 mL of 70%  
138 (wt/vol) sucrose in TE buffer layered with 10 ml of 53% (wt/vol) sucrose in TE buffer to form a gradient, and  
139 subjected to centrifugation at 4°C at 400,000 g for 5 h. The upper band (inner membrane proteins) and lower band  
140 (outer membrane proteins) were collected from the top of the gradient. After removing sucrose using a filter  
141 (Amicon Ultracel-3K; Millipore), the membrane fractions were solubilized in sodium dodecyl sulfate (SDS)  
142 sample buffer and were used for Western blot. Cells harboring pCA24N-*ompA* and pCA24N-*macB* prepared at  
143 the the same conditions were used as controls.

144 **Western blot analysis.** A total of a 2.5 µg protein was loaded and run using Tricine-SDS-PAGE as described  
145 previously (32). Proteins were transferred to a PVDF membrane (Millipore, Bedford, MA, USA) and a Western  
146 blot was performed with primary antibodies raised against the His tag (Cell Signaling Technology, Danvers, MA,  
147 USA) or GFP (Abmart, Shanghai, China) and horseradish peroxidase-conjugated goat anti-mouse secondary  
148 antibodies (Bio-Rad, Richmond, CA, USA).

149 **qRT-PCR.** Total RNA was isolated (33) using an RNA isolation kit (Invitrogen, Carlsbad, CA). DNase was  
150 applied during the RNA isolation process to avoid contamination of DNA. A total of 50 ng total RNA was used  
151 for qRT-PCR using the *Power SYBR<sup>®</sup> Green RNA-to-C<sub>1</sub><sup>™</sup> I-Step* Kit and the *StepOne<sup>™</sup> Real-Time PCR*  
152 *System* (Applied Biosystems). Primers were annealed at 60°C, and *rrsG* (34) was used to normalize the data.  
153 Relative expression levels of induction or repression of *elaB* under different conditions were calculated as  
154 described previously (35).

155 **Electrophoretic mobility shift assay (EMSA).** EMSAs were performed as previously described (36, 37). Briefly,  
156 DNA fragments were amplified using the primer pairs shown in **Table S1**. PCR products were gel purified with a  
157 QIAquick Gel Extraction Kit (Qiagen) and labeled with the Pierce<sup>™</sup> biotin 3' end DNA labeling kit (Thermo  
158 scientific, Rockford, IL). For the binding reactions, the *E. coli* RNA core polymerase (NEB, Ipswich, MA, USA)  
159 was mixed 1:2 (M:M) with RpoS at room temperature for 5 min to form the holoenzyme before the addition of  
160 biotin labeled DNA probes (0.05 pmol). The binding reaction was performed with the nonspecific competitor  
161 DNA (poly dI-dC) and NP-40 in buffer containing 10 mM HEPES (pH 7.3), 20 mM KCl, 1 mM MgCl<sub>2</sub>, and 5%  
162 glycerol at 25°C for 3 h. The final mixtures were run on a 6% DNA retardation gel (Invitrogen), transferred to a  
163 nylon membrane, and UV cross-linked. Chemiluminescence was performed with the LightShift  
164 Chemiluminescent EMSA Kit (Thermo Fisher Scientific, Rockford, IL, USA) according to the manufacturer's  
165 protocol.

166  **$\beta$ -galactosidase activity assay.** BW25113 wild-type and  $\Delta rpoS$  cells harboring pHGR01-*PelaB* or pHGR01-  
167 *MPelaB* were cultured to a turbidity at 600 nm of 6.0, and 800  $\mu$ L cultures were diluted with 4 mL PM2 (70 mM  
168 Na<sub>2</sub>HPO<sub>4</sub>·12H<sub>2</sub>O, 30 mM NaH<sub>2</sub>PO<sub>4</sub>·H<sub>2</sub>O, 1 mM MgSO<sub>4</sub> and 0.2 mM MnSO<sub>4</sub>, pH 7.0) (38). Then 30  $\mu$ L of  
169 toluene and 35  $\mu$ L of a 0.1% SDS solution were added to 2.5 mL of bacterial suspension to permeabilize cells.  
170 The mixtures were vortexed for 10 s and incubated at 37°C for 45 min in a water bath for evaporation of toluene.  
171 For the enzymatic reaction, 250  $\mu$ L of permeabilized cells was added to PM2 supplemented with  $\beta$ -  
172 mercaptoethanol (final concentration, 100 mM) to a final volume of 1 mL. The reaction was started by adding 250  
173  $\mu$ L of 4 mg/mL *o*-nitrophenol-galactoside in PM2. Then 500  $\mu$ L of 1M Na<sub>2</sub>CO<sub>3</sub> was added to stop the reaction  
174 and turbidity at 420 nm was measured. The  $\beta$ -galactosidase activity (Miller units) was calculated as described

175 previously (39). For *rpoS* complementation studies, cells carrying pCA24N-*rpoS* were cultured to a turbidity at  
176 600 nm 1.0 and expression of RpoS was induced with 0.5 mM IPTG for 2 h, and  $\beta$ -galactosidase activity was  
177 measured as above.

178 **Survival assay.** Overnight cultures were diluted to a turbidity at 600 nm of 0.05 in LB, and incubated at 37°C  
179 with 250 RPM shaking until cultures reached a turbidity of 1.0. Then 1 mL was collected for a cell viability assay  
180 to measure the initial population. For strains using pCA24N-based plasmids, overnight cultures were diluted to a  
181 turbidity of 0.05 and grown to a turbidity of 0.5, then 1 mM IPTG was used to induce gene expression for 2 h, and  
182 the turbidity was adjusted to 1.0 (34). For the oxidative stress assay, 1 mL cultures were treated with or without  
183 20 mM H<sub>2</sub>O<sub>2</sub> for 10 mins, and cells were serially diluted in 0.85% NaCl solution and applied as 10  $\mu$ L drops on  
184 LB agar. For the persistence assay, 100  $\mu$ g/mL ampicillin or 5.0  $\mu$ g/mL ciprofloxacin were added to cultures with  
185 a turbidity of 1.0, followed by incubation for 3 h; cell survival was determined by drop assay. For heat shock  
186 stress, cultures at a turbidity of 1.0 were transferred from 37°C to 65°C using a water shaking incubator for 5 min  
187 and 10 min.

188 **Determination of MICs.** MICs were determined using BIOFOSUN (Shanghai, China) drug-sensitive test plates.  
189 In brief, overnight cultures were diluted to turbidity of 0.05 in LB medium and incubated at 37°C until the  
190 turbidity reached 0.1. Cultures were diluted 1:100 in fresh LB medium and 100  $\mu$ l of the cell suspension  
191 inoculated into the wells which were treated with different concentrations of antibiotics. Then the cells were  
192 cultured without shaking for 20 h at 37°C. The MIC was determined as the lowest antibiotic concentrations with  
193 no visible growth occurred.

194 **Statistical Analysis.** Statistical analysis was performed using SPSS (16.0 version). The differences of the  
195 corresponding values among different conditions were tested by one-way analysis of variance (ANOVA)  
196 followed by a least significant difference test. A probability level (*p*-value) of less than 0.05 was regarded as  
197 statistically significant.

198

199

## RESULTS



200 **ElaB is an inner membrane protein with conserved C-terminal transmembrane domain.** ElaB is a small  
201 protein of 101 amino acids. It has one transmembrane domain at the C-terminus, and this domain is conserved in  
202 several bacterial species including opportunistic pathogens (**Figure 1**). In contrast, the N-terminus of these  
203 proteins shows much less conservation in terms of length and amino acid composition. Two proteins in *E. coli*,  
204 YqjD and YgaM, share the same C-terminal transmembrane domain of ElaB. Moreover, the transmembrane  
205 domain is very close to the end of the C-terminus and is followed by two to four residues containing one to three  
206 arginines (**Figure 1**).

207 ElaB localization in *E. coli* was first checked by fusing a red fluorescence protein gene *mCherry* to the C-  
208 terminal of the *elaB* gene in the chromosome of BW25113 wild-type cells to express the fused protein ElaB-  
209 mCherry. As expected, ElaB-mCherry was localized to the cell poles (**Figure 2, upper panel**). To exclude the  
210 potential effects of C-terminal mCherry on localization, we also fused the *mCherry* gene to the C-terminal of the  
211 *lacZ* gene in the chromosome of BW25113 wild-type cells, and the fused protein LacZ-mCherry was localized in  
212 the cytoplasm (**Figure 2, lower panel**). To further check the ElaB localization, ElaB with a green fluorescent  
213 protein (GFP) tagged at the C-terminus was produced using pCA24N-*elaB-gfp*. As expected, GFP-fused ElaB  
214 was also localized to the cell poles (**Figure S1**). Localization of GFP-fused membrane protein at the cell poles  
215 was also observed with previously characterized inner membrane proteins YqjD (40) and YidC (41), suggesting  
216 that ElaB should be anchored in the membrane.

217 To further determine ElaB resides in the inner membrane or outer membrane, the membrane proteins of *E.*  
218 *coli* were fractionated by a sucrose cushion protocol, which takes advantage of the fact that the inner membrane of  
219 *E. coli* has a lower density than the outer membrane (17, 31). Different cell fractions were obtained from *E. coli*  
220 producing ElaB with an N-terminal His-tag using plasmid pCA24N-*elaB*. A Western blot was conducted to detect  
221 the His-tagged ElaB in the membrane fractions using a His-tagged antibody. His-ElaB was only present in inner  
222 membrane fraction but not in the outer membrane fraction (**Figure 3A**, lanes 1-4). We also used inner membrane  
223 protein MacB (42) and outer membrane protein OmpA (43) as positive controls for membrane protein localization  
224 assay. As expected, MacB was found only in the inner membrane fraction (**Figure 3A**, lanes 5-8), while OmpA  
225 was largely present in the outer membrane fraction with a small proportion in the inner membrane fraction due to

226 its high abundance (44) (**Figure 3A**, lanes 9-12).

227 A previous study showed that both YqjD and ElaB are ribosome-associated proteins and YqjD is also  
228 anchored in the inner membrane (17). To see whether there is possibility that some of the ribosome-associated  
229 protein ElaB is also present in the soluble fraction, we quantified the levels of GFP-fused ElaB in the soluble and  
230 the membrane fractions. More than 90% of the ElaB expressed by pCA24N-*elaB* in the whole cell lysate could be  
231 recovered in the membrane fraction with a small proportion present in the soluble fraction (**Figure 3B**, lanes 1-3).  
232 Similar results were obtained using GFP-fused ElaB integrated in the chromosome of BW25113 wild-type  
233 (**Figure 3B**, lanes 4-6). In *E. coli*, ribosomes translating membrane proteins interact cotranslationally with  
234 translocons in the membrane, a process that is essential for proper insertion of nascent polypeptides into the  
235 membrane (9). Here, we demonstrate that ElaB, which shares a conserved transmembrane motif with YqjD, is  
236 also an inner membrane protein. Unlike YqjD, production of ElaB did not inhibit cell growth or lead to cell lysis  
237 (data not shown).

238 ***elaB* is regulated by RpoS.** To determine when ElaB is induced, we first examined *elaB* expression during  
239 different growth conditions. Transcription of *elaB* was up-regulated  $13.9 \pm 0.2$  fold when cells entered the  
240 stationary phase, and transcription of *elaB* was also up-regulated  $9.5 \pm 0.6$  fold when cells were growing in  
241 nutrient-limited minimal medium (M9 minimal medium with 0.4% glucose) compared to LB medium during the  
242 exponential growing phase (**Figure 4A**). By contrast, expression of the neighboring upstream gene *elaA* did not  
243 change during these growth conditions (data not shown).

244 To test whether expression of *elaB* is under the direct control of the stationary sigma factor RpoS ( $\sigma^{38}$ ), *elaB*  
245 expression was first tested in an *rpoS* deletion mutant. As expected, there was no induction of *elaB* in the absence  
246 of RpoS in the stationary phase (**Figure 4B**). Moreover, transcription of *elaB* was up-regulated  $2.4 \pm 0.1$  fold by  
247 overexpressing *rpoS* via pCA24N-*rpoS* in minimal medium during the exponential growing phase (**Figure 4B**).  
248 Next, Virtual Footprint (45) and FGENESB (Softberry, <http://www.softberry.com>) programs were applied to  
249 predict potential RpoS binding sites in the *elaB* promoter. Two RpoS binding sites were identified at 65 nt and  
250 401 nt upstream of the start codon of *elaB*, respectively (**Figure 4C**). The predicted binding sites were also  
251 aligned with previous identified consensus sequences for RpoS regulon (37, 46-51), and -10 region in the putative

252 RpoS binding site 2 close to *elaB* start codon showed high similarity to the previously proposed -10 region  
253 consensus sequence of TGN<sub>0-2</sub>CYATAMT (Y stands for C or T and M stands for A or C) (48) or CTATA(c/a)T  
254 (50). Moreover, -35 region is 18 nucleotides away from the -10 region in the putative RpoS binding site 2, which  
255 is regarded as a functional location ( $17 \pm 2$  nucleotides) (51).

256 To determine how RpoS regulates *elaB* transcription, we conducted EMSA with two DNA probes amplified  
257 from the promoter of *elaB* (Probe 1 containing putative RpoS binding site 1 and Probe 2 containing putative RpoS  
258 binding site 2) using purified RpoS (**Figure 3D**) in the presence of *E. coli* core RNA polymerase. As shown in  
259 **Figure 4EF**, RpoS only bound and shifted the DNA fragment containing the RpoS binding site close to *elaB* start  
260 codon (Probe 2) in a dose dependent manner, but did not bind or shift the DNA fragment containing the RpoS  
261 binding site 1 (Probe 1), as well as the mutant RpoS binding site 2 (Probe 3) (**Figure 4C**).

262 To further confirm the regulation of RpoS *in vivo*, we conducted promoter activity assays by fusing the  
263 promoter of *elaB* with the *lacZ* gene in pHGR01 to construct the *lacZ* reporter plasmid pHGR01-*PelaB*. As  
264 expected, the BW25113 wild-type cells harboring pHGR01-*PelaB* showed significantly higher  $\beta$ -galactosidase  
265 activity ( $1034.2 \pm 34.2$  miller units, MU) than the  $\Delta rpoS$  cells ( $268.9 \pm 15.9$  MU) (**Figure 5A**). Moreover, we  
266 performed site-mutagenesis to change the conserved RpoS binding site from TTCAGG (-35  
267 region)...TCTATAGTTA (-10 region) to AAAAAA (-35 region)...CCCCCCCC (-10 region) (**Figure 4C**) in  
268 pHGR01-*PelaB* to construct a mutant *lacZ* reporter plasmid pHGR01-M*PelaB*. Both the wild-type and  $\Delta rpoS$   
269 hosts carrying pHGR01-M*PelaB* had similar  $\beta$ -galactosidase activities, suggesting that RpoS no longer regulates  
270 the *elaB* transcription once the conserved binding site is altered (**Figure 5A**). To further confirm the regulation of  
271 RpoS on *elaB*, we conducted the complementation experiment of the promoter activity assay by using pCA24N-  
272 *rpoS* to overexpress *rpoS* in the  $\Delta rpoS$  host cells. As expected, using pHGR01-*PelaB* as the reporter plasmid,  
273  $\Delta rpoS$  cells overexpressing *rpoS* via pCA24N-*rpoS* showed  $8.0 \pm 0.9$ -fold increase in the promoter activity as  
274 compared to the empty plasmid pCA24N ( $937.6 \pm 101.5$  MU for  $\Delta rpoS$ /pCA24N-*rpoS* versus  $117.3 \pm 4.0$  MU for  
275  $\Delta rpoS$ /pCA24N). However, when pHGR01-M*PelaB* was used as the reporter plasmid, the activity of the mutated  
276 promoter of *elaB* did not change in the  $\Delta rpoS$  cells overexpressing *rpoS* or not ( $70.4 \pm 6.7$  MU for  
277  $\Delta rpoS$ /pCA24N-*rpoS* versus  $83.7 \pm 6.2$  MU for  $\Delta rpoS$ /pCA24N) (**Figure 5B**). Collectively, these results

278 demonstrate that *elaB* is induced in the stationary phase, and transcription of *elaB* is under the direct control of  
279 stationary phase sigma factor RpoS.

280 **ElaB increases survival during heat and oxidative stress.** To determine the physiological role of ElaB, we  
281 tested whether *elaB* contributes to survival under stressed conditions using the *elaB* deletion mutant. To test  
282 whether ElaB contributes to survival under heat shock, cell viability was determined with and without *elaB* at  
283 65°C for 10 min. Survival was greatly reduced  $(3.3 \pm 0.1) \times 10^5$ -fold when *elaB* was deleted (**Figure 6A**), and  
284 complementation of the *elaB* mutation increased survival upon heat shock (**Figure 6B**). Similarly, cell survival  
285 after treatment with 20 mM H<sub>2</sub>O<sub>2</sub> for 10 min was reduced approximately  $3.6 \times 10^4$ -fold when *elaB* was deleted  
286 (**Figure 6C**), and complementation of *elaB* mutation increased cell viability  $1.2 \times 10^5$ -fold to levels similar to the  
287 wild-type (**Figure 6D**). Collectively, these results show that ElaB increases oxidative and heat stress resistance.

288 **ElaB decreases persister cell formation.** Inner membrane proteins can mediate antibiotic resistance as well as  
289 persister cell formation either by damaging the cell membrane or affecting membrane permeability (52-56).  
290 Persister cells are phenotypic variants of regular cells, play a major role in the high antibiotic resistance of  
291 bacterial biofilms, and are likely responsible for the recalcitrance of chronic infections to antibiotics (57-59). To  
292 investigate the role of ElaB in persister cell formation, we first measured the MICs (minimal inhibitory  
293 concentrations) of ten commonly used antibiotics for bacterial infections for the  $\Delta$ *elaB* strain and the wild-type  
294 strain. As shown in **Table 2**, changes of MIC values of the ten antibiotics between the two strains were within  
295 two-fold. Next, we performed the persister cell assay using high concentrations ( $>10 \times$ MIC) of ampicillin and  
296 ciprofloxacin. The numbers of persister cells formed in the  $\Delta$ *elaB* strain were  $4.3 \pm 0.5$  fold higher after 1 h, and  
297  $12.6 \pm 0.5$  fold higher after 3 h when treated with 100  $\mu$ g/mL ampicillin (**Figure 7A**). Critically, persister cell  
298 formation in the  $\Delta$ *elaB* strain was  $(1.15 \pm 0.1) \times 10^3$ -fold higher than the wild-types cells, when treated with 5  
299  $\mu$ g/mL ciprofloxacin for 1 h. After 3 h, no persister cells was detected in the wild-type strain, while the proportion  
300 of persister cell in the  $\Delta$ *elaB* cells was  $0.06 \pm 0.01\%$  (**Figure 7B**). Similar to what has been reported earlier (60),  
301 ciprofloxacin appears to be more effective in killing regular non-growing cells compared to ampicillin.  
302 Additionally, complementation of *elaB* via pCA24N-*elaB* reduced the persister cell formation when compared to  
303  $\Delta$ *elaB* cells harboring an empty pCA24N plasmid (**Figure 7CD**). Collectively, these results suggest that the

304 inactivation of ElaB greatly increases persister cell formation.

## 305 DISCUSSION

306 Bacterial membranes play essential roles in the response to various stresses. Here we identified a new small  
307 inner membrane protein with a C-terminal transmembrane domain in *E.coli*, ElaB, which has a role in multiple  
308 stress responses. We found that (i) Expression of *elaB* is up-regulated during the stationary phase, and it is  
309 positively regulated by RpoS in a concentration dependent manner by the binding of RpoS to the *elaB* promoter;  
310 (ii) ElaB protects cells against oxidative stress and heat shock; and (iii) ElaB decreases persister cell formation. C-  
311 tail anchored inner membrane proteins were first identified in eukaryotes, and have been shown to play critical  
312 roles in apoptosis and other vital processes (10-12). In *Streptomyces coelicolor*, they may also play an important  
313 role (61). Here we provide evidence that the C-tail anchored inner membrane protein ElaB in *E. coli* participates  
314 in important cellular processes such as the response to heat stress and oxidative stress.

315 Sigma factor RpoS is a general stress response regulator, and in *E. coli*, environmental stresses such as  
316 oxidative stress, stimulate the expression of the *rpoS* gene and thus turn on the expression of the RpoS-controlled  
317 regulon (22, 62, 63). Transcription of genes recognized by RpoS through specific sequences in the promoter  
318 allows the activation of a 'general stress response', thus protecting cells from harmful conditions (51). In this  
319 study, we showed that the previously uncharacterized ElaB is under the direct control of RpoS, and ElaB protects  
320 cells fight against oxidative stress. Thus, under stressed condition where RpoS is up-regulated (22), *elaB*  
321 transcription should also be induced, illustrating another example of the multifactorial regulation of RpoS. In  
322 addition, the upregulation of *elaB* by RpoS has been also previously detected by other groups using DNA  
323 microarray studies under stressed conditions (62, 64, 65). Deletion of *rpoS*, as well as the genes that RpoS  
324 controls, increases *E. coli* persister formation dramatically to the extent that nearly the whole population became  
325 persistent (66). Moreover, biofilms of the *rpoS* mutant were much more resistant to killing by tobramycin than  
326 were wild-type *P. aeruginosa* biofilms (67). However, the underlying mechanism is unclear. Here we found that  
327 ElaB, activated by RpoS, greatly decreased tolerance to high concentrations of ciprofloxacin by forming more  
328 persister cells. Other two identified C-terminal anchored membrane proteins, YqjD and YgaM, are also induced in  
329 the stationary phase in *E.coli* (17). However, the physiological functions of both YgaM and YqjD are largely

330 unknown except that YqjD has been suggested to inhibit cell growth by the inactivation of translational properties  
331 of ribosomes (17). We previously found that deletion of the acid stress related genes (e.g., *gadB*) that are  
332 activated by RpoS (64) or its transcriptional activator *gadX* greatly increased persister cells formation (66).  
333 Nevertheless, these results suggest that the RpoS and genes under the direct control of RpoS are potentially  
334 important for the general stress response, but the underlying mechanism of how these genes contribute to the  
335 reduction of tolerance to high concentrations of antibiotic while maintaining enhanced resistance to non-antibiotic  
336 environmental stresses needs further investigation. Thus, disruption of C-tail anchored inner membrane proteins  
337 can reduce stress resistance; it can also lead to deleterious effects such as increased persistence in *E. coli*.

338 Our blast search indicates that ElaB, as well as YqjD and YgaM, lack N-terminal signal sequences. The high  
339 diversity of the N-terminal domains of these proteins, which exhibit no universally conserved sequence  
340 characteristics, argues for a membrane targeting mechanism that depends primarily, if not entirely on, the C-  
341 terminal domains. Although the ‘twin-arginine repeat’ or TAT pathway is involved in the secretion of folded  
342 proteins (68) and ElaB has two arginines at the end of the C terminus, it lacks the characteristic Z-R-R- $\phi$ -X-X  
343 sequence (where Z is a polar residues, X-X are hydrophobic residues and  $\phi$  is any residue) recognized by the TAT  
344 system (**Figure 1**). Hence, it is unlikely that ElaB is secreted by the TAT system. In the absence of their N-  
345 terminal signal sequence, the C-terminal transmembrane domain of these C-tail anchored proteins identified in *S.*  
346 *coelicolor* is sufficient for membrane targeting (13). However, the underlying targeting pathways has not been  
347 elucidated. The identification of this new targeting pathway suggests it may be an important target for  
348 antimicrobial agents.

349 Two small hydrophobic polypeptides TisB (53) and GhoT (52, 54, 69) are toxin components of toxin-  
350 antitoxin systems. They both are not under the regulation of RpoS, and are found to increase persister cell  
351 formation by reducing cell metabolism to create dormancy. GhoT is a small membrane proteins with two  
352 transmembrane domains (residues 7 to 27 and 37 to 57) (52). Additionally, TisB (53) and GhoT damage cell  
353 envelopes and lead to cell death when overproduced, but overproduction of ElaB did not cause growth inhibition,  
354 indicating that different inner membrane proteins and transmembrane proteins may function differently in the  
355 presence of general stress. By using *in vivo* fluorescent imaging and next-generation sequencing, bacterial

356 persister cells, in addition to dormancy (70), employ an “active defense” to pump antibiotics out and reduce  
357 intracellular drug concentrations through enhanced efflux activity (55). Since ElaB does not seem to affect the  
358 metabolic state of the cell, it is possible that the function of ElaB is involved with efflux pumps either by  
359 enhanced pumping out the antibiotic to the outside of the cell or by limiting the uptake of the antibiotic. Although  
360 the C-terminal transmembrane domain of ElaB and YqjD is highly conserved, the function of ElaB and YqjD  
361 seem different. YqjD inhibits cell growth by binding to the 30S subunit of in the 70S and 100S ribosomes at the  
362 N-terminal region (17). However, the N-terminal regions of these two proteins are not highly conserved, and  
363 overproduction of ElaB does not lead to growth inhibition or cell lysis. Future studies are needed to elucidate the  
364 biochemical properties of these C-tailed inner membrane proteins and how they interact with efflux pumps or  
365 other cellular components in prokaryotes.

366

#### ACKNOWLEDGEMENTS

367 We are grateful for the Keio and ASKA strains provided by the Genome Analysis Project in Japan.

368

#### FUNDING INFORMATION

369 This work was supported by the National Science Foundation of China (Grant No. 31290233, 31625001 and  
370 31500025), by National Science Foundation of Guangdong Province (2015A030310405), China Postdoctoral  
371 Science Foundation funded project (2013M542217 and 2014T70830) and by the Army Research Office  
372 (W911NF-14-1-0279). XW is a recipient of the 1000-Youth Elite Program (the Recruitment Program of Global  
373 Experts in China).

374

#### COMPETING FINANCIAL INTERESTS

375 The authors declare no competing financial interests.

376

## REFERENCES

- 377 1. **Krogh A, Larsson B, von Heijne G, Sonnhammer ELL.** 2001. Predicting  
378 transmembrane protein topology with a hidden Markov model: Application to  
379 complete genomes. *J Mol Biol* **305**:567-580.
- 380 2. **Liszewski K.** 2015. Dissecting the structure of membrane proteins.
- 381 3. **Koebnik R, Locher KP, Van Gelder P.** 2000. Structure and function of bacterial  
382 outer membrane proteins: barrels in a nutshell. *Mol Microbiol* **37**:239-253.
- 383 4. **Saier MH, Jr., Reddy VS, Tsu BV, Ahmed MS, Li C, Moreno-Hagelsieb G.**  
384 2016. The transporter classification database (TCDB): recent advances. *Nucleic*  
385 *Acids Res* **44**:D372-379.
- 386 5. **Shen K, Shan SO.** 2010. Transient tether between the SRP RNA and SRP receptor  
387 ensures efficient cargo delivery during cotranslational protein targeting. *Proc Natl*  
388 *Acad Sci U S A* **107**:7698-7703.
- 389 6. **Moffitt JR, Pandey S, Boettiger AN, Wang SY, Zhuang XW.** 2016. Spatial  
390 organization shapes the turnover of a bacterial transcriptome. *Elife* **5**.
- 391 7. **Kol S, Nouwen N, Driessen AJ.** 2008. Mechanisms of YidC-mediated insertion  
392 and assembly of multimeric membrane protein complexes. *J Biol Chem* **283**:31269-  
393 31273.
- 394 8. **Johnson AE, van Waes MA.** 1999. The translocon: A dynamic gateway at the ER  
395 membrane. *Annu Rev Cell Dev Bi* **15**:799-842.
- 396 9. **Herskovits AA, Bibi E.** 2000. Association of *Escherichia coli* ribosomes with the  
397 inner membrane requires the signal recognition particle receptor but is independent  
398 of the signal recognition particle. *Proc Natl Acad Sci U S A* **97**:4621-4626.
- 399 10. **Kalbfleisch T, Cambon A, Wattenberg BW.** 2007. A bioinformatics approach to  
400 identifying tail-anchored proteins in the human genome. *Traffic* **8**:1687-1694.
- 401 11. **Pedrazzini E.** 2009. Tail-Anchored Proteins in Plants. *J Plant Biol* **52**:88-101.
- 402 12. **Kriechbaumer V, Shaw R, Mukherjee J, Bowsher CG, Harrison AM, Abell**  
403 **BM.** 2009. Subcellular distribution of tail-anchored proteins in arabidopsis. *Traffic*  
404 **10**:1753-1764.
- 405 13. **Craney A, Tahlan K, Andrews D, Nodwell J.** 2011. Bacterial transmembrane  
406 proteins that lack N-terminal signal sequences. *Plos One* **6**.
- 407 14. **Borgese N, Righi M.** 2010. Remote origins of tail-anchored proteins. *Traffic*  
408 **11**:877-885.
- 409 15. **Karlinsey JE, Pease AJ, Winkler ME, Bailey JL, Hughes KT.** 1997. The *flk* gene  
410 of *Salmonella typhimurium* couples flagellar P- and L-ring assembly to flagellar  
411 morphogenesis. *J Bacteriol* **179**:2389-2400.
- 412 16. **Frost LS, Paranchych W, Willetts NS.** 1984. DNA-sequence of the F-traale region  
413 that includes the gene for F-pilin. *J Bacteriol* **160**:395-401.
- 414 17. **Yoshida H, Maki Y, Furuike S, Sakai A, Ueta M, Wada A.** 2012. YqjD is an  
415 inner membrane protein associated with stationary-phase ribosomes in *Escherichia*  
416 *coli*. *J Bacteriol* **194**:4178-4183.
- 417 18. **Luirink J, Yu Z, Wagner S, de Gier JW.** 2012. Biogenesis of inner membrane  
418 proteins in *Escherichia coli*. *BBA-Bioenergetics* **1817**:965-976.
- 419 19. **Farr SB, Kogoma T.** 1991. Oxidative stress responses in *Escherichia coli* and  
420 *Salmonella typhimurium*. *Microbiol Rev* **55**:561-585.



- 421 20. **Jara LM, Cortes P, Bou G, Barbe J, Aranda J.** 2015. Differential roles of  
422 antimicrobials in the acquisition of drug resistance through activation of the SOS  
423 response in *Acinetobacter baumannii*. *Antimicrob Agents Ch* **59**:4318-4320.
- 424 21. **Spaniol V, Bernhard S, Aebi C.** 2015. *Moraxella catarrhalis* AcrAB-OprM efflux  
425 pump contributes to antimicrobial resistance and is enhanced during cold shock  
426 response. *Antimicrob Agents Ch* **59**:1886-1894.
- 427 22. **Battesti A, Majdalani N, Gottesman S.** 2011. The RpoS-mediated general stress  
428 response in *Escherichia coli*. *Annu Rev Microbiol* **65**:189-213.
- 429 23. **Dutta T, Deutscher MP.** 2009. Catalytic properties of RNase BN/RNase Z from  
430 *Escherichia coli*: RNase BN is both an exo- and endonuclease. *J Biol Chem*  
431 **284**:15425-15431.
- 432 24. **Asha PK, Blouin RT, Zaniewski R, Deutscher MP.** 1983. Ribonuclease BN:  
433 identification and partial characterization of a new tRNA processing enzyme. *Proc*  
434 *Natl Acad Sci U S A* **80**:3301-3304.
- 435 25. **Catic A, Misaghi S, Korbelt GA, Ploegh HL.** 2007. ElaD, a deubiquitinating  
436 protease expressed by *E. coli*. *PLoS ONE* **2**:e381.
- 437 26. **Maniatis T, Sambrook J, Fritsch EF.** 1989. *Molecular cloning: A laboratory*  
438 *manual*, 2nd ed. Cold Spring Harbor Laboratory Press Cold Spring Harbor, N.Y.
- 439 27. **Wang X, Kim Y, Ma Q, Hong SH, Pokusaeva K, Sturino JM, Wood TK.** 2010.  
440 Cryptic prophages help bacteria cope with adverse environments. *Nat Commun*  
441 **1**:147.
- 442 28. **Baba T, Ara T, Hasegawa M, Takai Y, Okumura Y, Baba M, Datsenko KA,**  
443 **Tomita M, Wanner BL, Mori H.** 2006. Construction of *Escherichia coli* K-12 in-  
444 frame, single-gene knockout mutants: the Keio collection. *Mol Syst Biol*  
445 **2**:2006.0008.
- 446 29. **Kitagawa M, Ara T, Arifuzzaman M, Ioka-Nakamichi T, Inamoto E, Toyonaga**  
447 **H, Mori H.** 2005. Complete set of ORF clones of *Escherichia coli* ASKA library (A  
448 complete set of *E. coli* K-12 ORF archive): Unique resources for biological  
449 research. *DNA Res* **12**:291-299.
- 450 30. **Datsenko KA, Wanner BL.** 2000. One-step inactivation of chromosomal genes in  
451 *Escherichia coli* K-12 using PCR products. *Proc Natl Acad Sci U S A* **97**:6640-  
452 6645.
- 453 31. **Castanie-Cornet MP, Cam K, Jacq A.** 2006. RcsF is an outer membrane  
454 lipoprotein involved in the RcsCDB phosphorelay signaling pathway in *Escherichia*  
455 *coli*. *J Bacteriol* **188**:4264-4270.
- 456 32. **Schägger H.** 2006. Tricine-SDS-PAGE. *Nat Protocols* **1**:16-22.
- 457 33. **Ren D, Bedzyk LA, Thomas SM, Ye RW, Wood TK.** 2004. Gene expression in  
458 *Escherichia coli* biofilms. *Appl Microbiol Biotechnol* **64**:515-524.
- 459 34. **Wang X, Kim Y, Hong SH, Ma Q, Brown BL, Pu M, Tarone AM, Benedik MJ,**  
460 **Peti W, Page R, Wood TK.** 2011. Antitoxin MqsA helps mediate the bacterial  
461 general stress response. *Nat Chem Biol* **7**:359-366.
- 462 35. **Guo Y, Quiroga C, Chen Q, McAnulty MJ, Benedik MJ, Wood TK, Wang X.**  
463 2014. RalR (a DNase) and RalA (a small RNA) form a type I toxin-antitoxin system  
464 in *Escherichia coli*. *Nucleic Acids Res* **42**:6448-6462.
- 465 36. **Zhao K, Liu M, Burgess RR.** 2005. The global transcriptional response of  
466 *Escherichia coli* to induced sigma 32 protein involves sigma 32 regulon activation

- 467 followed by inactivation and degradation of sigma 32 *in vivo*. J Biol Chem  
468 **280**:17758-17768.
- 469 37. **Lee SJ, Gralla JD.** 2001. Sigma38 (*rpoS*) RNA polymerase promoter engagement  
470 via-10 region on nucleotides. J Biol Chem **276**:30064-30071.
- 471 38. **Karimova G, Dautin N, Ladant D.** 2005. Interaction network among *Escherichia*  
472 *coli* membrane proteins involved in cell division as revealed by bacterial two-hybrid  
473 analysis. J Bacteriol **187**:2233-2243.
- 474 39. **Frias JE, Flores E.** 2015. Induction of the Nitrate Assimilation nirA Operon and  
475 Protein-Protein Interactions in the Maturation of Nitrate and Nitrite Reductases in  
476 the *Cyanobacterium Anabaena* sp Strain PCC 7120. J Bacteriol **197**:2442-2452.
- 477 40. **Li G, Young KD.** 2012. Isolation and identification of new inner membrane-  
478 associated proteins that localize to cell poles in *Escherichia coli*. Mol Microbiol  
479 **84**:276-295.
- 480 41. **Urbanus ML, Fröderberg L, Drew D, Björk P, de Gier J-WL, Brunner J,**  
481 **Oudega B, Luirink J.** 2002. Targeting, insertion, and localization of *Escherichia*  
482 *coli* YidC. J Biol Chem **277**:12718-12723.
- 483 42. **Daley DO, Rapp M, Granseth E, Melén K, Drew D, Von Heijne G.** 2005. Global  
484 topology analysis of the *Escherichia coli* inner membrane proteome. Science  
485 **308**:1321-1323.
- 486 43. **Freudl R, Schwarz H, Stierhof Y, Gamon K, Hindennach I, Henning U.** 1986.  
487 An outer membrane protein (OmpA) of *Escherichia coli* K-12 undergoes a  
488 conformational change during export. J Biol Chem **261**:11355-11361.
- 489 44. **Fontaine F, Fuchs RT, Storz G.** 2011. Membrane localization of small proteins in  
490 *Escherichia coli*. J Biol Chem **286**:32464-32474.
- 491 45. **Münch R, Hiller K, Grote A, Scheer M, Klein J, Schobert M, Jahn D.** 2005.  
492 Virtual Footprint and PRODORIC: an integrative framework for regulon prediction  
493 in prokaryotes. Bioinformatics:4187-4189.
- 494 46. **Peano C, Wolf J, Demol J, Rossi E, Petiti L, De Bellis G, Geiselmann J, Egli T,**  
495 **Lacour S, Landini P.** 2015. Characterization of the *Escherichia coli* sigma(S) core  
496 regulon by Chromatin Immunoprecipitation-sequencing (ChIP-seq) analysis. Sci  
497 Rep **5**.
- 498 47. **Maciag A, Peano C, Pietrelli A, Egli T, De Bellis G, Landini P.** 2011. In vitro  
499 transcription profiling of the sigmaS subunit of bacterial RNA polymerase: re-  
500 definition of the sigmaS regulon and identification of sigmaS-specific promoter  
501 sequence elements. Nucleic Acids Res **39**:5338-5355.
- 502 48. **Lacour S, Landini P.** 2004. sigma(S)-dependent gene expression at the onset of  
503 stationary phase in *Escherichia coli*: Function of sigma(S)-dependent genes and  
504 identification of their promoter sequences. J Bacteriol **186**:7186-7195.
- 505 49. **Typas A, Hengge R.** 2006. Role of the spacer between the-35 and-10 regions in  
506 sigma(s) promoter selectivity in *Escherichia coli*. Mol Microbiol **59**:1037-1051.
- 507 50. **Gaal T, Ross W, Estrem ST, Nguyen LH, Burgess RR, Gourse RL.** 2001.  
508 Promoter recognition and discrimination by EsigmaS RNA polymerase. Mol  
509 Microbiol **42**:939-954.
- 510 51. **Landini P, Egli T, Wolf J, Lacour S.** 2014. sigmaS, a major player in the response  
511 to environmental stresses in *Escherichia coli*: role, regulation and mechanisms of  
512 promoter recognition. Env Microbiol Rep **6**:1-13.

- 513 52. **Wang X, Lord DM, Cheng H-Y, Osbourne DO, Hong SH, Sanchez-Torres V,**  
514 **Quiroga C, Zheng K, Herrmann T, Peti W, Benedik MJ, Page R, Wood TK.**  
515 2012. A new type V toxin-antitoxin system where mRNA for toxin GhoT is cleaved  
516 by antitoxin GhoS. *Nat Chem Biol* **8**:858-861.
- 517 53. **Dörr T, Vulić M, Lewis K.** 2010. Ciprofloxacin causes persister formation by  
518 inducing the TisB toxin in *Escherichia coli*. *PLoS Biol* **8**:e1000317.
- 519 54. **Cheng HY, Soo VW, Islam S, McAnulty MJ, Benedik MJ, Wood TK.** 2014.  
520 Toxin GhoT of the GhoT/GhoS toxin/antitoxin system damages the cell membrane  
521 to reduce adenosine triphosphate and to reduce growth under stress. *Environ*  
522 *Microbiol* **16**:1741-1754.
- 523 55. **Pu YY, Zhao ZL, Li YX, Zou J, Ma Q, Zhao YN, Ke YH, Zhu Y, Chen HY,**  
524 **Baker MAB, Ge H, Sun YJ, Xie XS, Bai F.** 2016. Enhanced efflux activity  
525 facilitates drug tolerance in dormant bacterial cells. *Mol Cell* **62**:284-294.
- 526 56. **Gerdes K, Semsey S.** 2016. Pumping persisters. *Nature* **534**:41-42.
- 527 57. **Wood TK, Knabel SJ, Kwan BW.** 2013. Bacterial persister cell formation and  
528 dormancy. *Appl Environ Microbiol* **79**:7116-7121.
- 529 58. **del Pozo JL, Patel R.** 2007. The challenge of treating biofilm-associated bacterial  
530 infections. *Clin Pharmacol Ther* **82**:204-209.
- 531 19. **Lewis K.** 2007. Persister cells, dormancy and infectious disease. *Nat Rev Microbiol*  
532 **5**:48-56.
- 533 60. **Keren I, Kaldalu N, Spoering A, Wang Y, Lewis K.** 2004. Persister cells and  
534 tolerance to antimicrobials. *FEMS Microbiol Lett* **230**:13-18.
- 535 61. **Caraney A.** 2012. Small molecule interrogation of *Streptomyces coelicolor* growth,  
536 development and secondary metabolism. Doctor thesis:155.
- 537 62. **Weber H, Polen T, Heuveling J, Wendisch VF, Hengge R.** 2005. Genome-wide  
538 analysis of the general stress response network in *Escherichia coli*:  $\sigma^S$ -dependent  
539 genes, promoters, and sigma factor selectivity. *J Bacteriol* **187**:1591-1603.
- 540 63. **Hengge R.** 2009. Proteolysis of sigma(S) (RpoS) and the general stress response in  
541 *Escherichia coli*. *Res Microbiol* **160**:667-676.
- 542 64. **Patten CL, Kirchhof MG, Schertzberg MR, Morton RA, Schellhorn HE.** 2004.  
543 Microarray analysis of RpoS-mediated gene expression in *Escherichia coli* K-12.  
544 *Mol Genet Genomics* **272**:580-591.
- 545 65. **Ito A, May T, Kawata K, Okabe S.** 2008. Significance of *rpoS* during maturation  
546 of *Escherichia coli* biofilms. *Biotechnol Bioeng* **99**:1462-1471.
- 547 66. **Hong SH, Wang XX, O'Connor HF, Benedik MJ, Wood TK.** 2012. Bacterial  
548 persistence increases as environmental fitness decreases. *Microb Biotechnol* **5**:509-  
549 522.
- 550 67. **Whiteley M, Bangera MG, Bumgarner RE, Parsek MR, Teltzel GM, Lory S,**  
551 **Greenberg EP.** 2001. Gene expression in *Pseudomonas aeruginosa* biofilms.  
552 *Nature* **413**:860-864.
- 553 68. **Lee PA, Tullman-Ercek D, Georgiou G.** 2006. The bacterial twin-arginine  
554 translocation pathway. *Annu Rev Microbiol* **60**:373-395.
- 555 69. **Wang X, Lord DM, Hong SH, Peti W, Benedik MJ, Page R, Wood TK.** 2013.  
556 Type II toxin/antitoxin MqsR/MqsA controls type V toxin/antitoxin GhoT/GhoS.  
557 *Environ Microbiol* **15**:1734-1744.

- 558 70. **Rotem E, Loinger A, Ronin I, Levin-Reisman I, Gabay C, Shores N, Biham O,**  
559 **Balaban NQ.** 2010. Regulation of phenotypic variability by a threshold-based  
560 mechanism underlies bacterial persistence. *Proc Natl Acad Sci U S A* **107**:12541-  
561 12546.
- 562 71. **Fu HH, Jin M, Ju LL, Mao YT, Gao HC.** 2014. Evidence for function  
563 overlapping of CymA and the cytochrome bc(1) complex in the *Shewanella*  
564 *oneidensis* nitrate and nitrite respiration. *Environ Microbiol* **16**:3181-3195.
- 565

566 **Table 1.** Bacterial strains and plasmids used in this study. Cm<sup>R</sup> and Km<sup>R</sup> indicate chloramphenicol  
 567 and kanamycin resistance, respectively. P and MP indicate promoter and mutant promoter,  
 568 respectively.  
 569

Bacterial strains/Plasmids	Description	Source
<b>BW25113 <i>E. coli</i> K12 strains</b>		
wild-type	<i>lacI</i> <sup>f</sup> <i>rrnB</i> <sub>T14</sub> $\Delta$ <i>lacZ</i> <sub>WJ16</sub> <i>hsdR514</i> $\Delta$ <i>araBAD</i> <sub>AH33</sub> $\Delta$ <i>rhaBAD</i> <sub>LD78</sub> <i>rph</i> -	(28)
$\Delta$ <i>elaB</i>	$\Delta$ <i>elaB</i> $\Delta$ km <sup>R</sup>	(28)
$\Delta$ <i>rpoS</i>	$\Delta$ <i>rpoS</i> $\Delta$ km <sup>R</sup>	(28)
<i>elaB</i> :: <i>mCherry</i>	<i>mCherry</i> was fused before <i>elaB</i> stop codon in wild-type strain	this study
<i>lacZ</i> :: <i>mCherry</i>	<i>mCherry</i> was fused before <i>lacZ</i> stop codon in wild-type strain	this study
<i>elaB</i> :: <i>gfp</i>	<i>gfp</i> was fused before <i>elaB</i> stop codon in wild-type strain	this study
<b>Plasmids</b>		
pCA24N	Cm <sup>R</sup> ; <i>lacI</i> <sup>f</sup> ,	(29)
pCA24N- <i>elaB</i>	Cm <sup>R</sup> ; <i>lacI</i> <sup>f</sup> , P <sub>T5-lac</sub> :: <i>elaB</i>	(29)
pCA24N- <i>gfp</i>	Cm <sup>R</sup> ; <i>lacI</i> <sup>f</sup> , with <i>gfp</i> gene	(29)
pCA24N- <i>elaB-gfp</i>	Cm <sup>R</sup> ; <i>lacI</i> <sup>f</sup> , P <sub>T5-lac</sub> :: <i>elaB</i> , with <i>gfp</i> gene	(29)
pCA24N- <i>ompA</i>	Cm <sup>R</sup> ; <i>lacI</i> <sup>f</sup> , P <sub>T5-lac</sub> :: <i>ompA</i>	(29)
pCA24N- <i>macB</i>	Cm <sup>R</sup> ; <i>lacI</i> <sup>f</sup> , P <sub>T5-lac</sub> :: <i>macB</i>	(29)
pCA24N- <i>rpoS</i>	Cm <sup>R</sup> ; <i>lacI</i> <sup>f</sup> , P <sub>T5-lac</sub> :: <i>rpoS</i>	(29)
pET28b- <i>rpoS</i>	Km <sup>R</sup> ; <i>lacI</i> <sup>f</sup> , pET28b P <sub>T7-lac</sub> :: <i>rpoS</i> with C-terminal His-tagged	this study
pHGR01	Km <sup>f</sup> , R6K <i>ori</i> , promoterless- <i>lacZ</i> reporter vector	(71)
pHGR01- <i>PelaB</i>	Fused <i>elaB</i> promoter with <i>lacZ</i> in pHGR01	this study
pHGR01-MP <i>elaB</i>	RpoS binding site in <i>elaB</i> promoter was mutant as pointed	this study

570  
 571

572  
573  
574**Table 2.** MICs (minimal inhibitory concentrations) of wild-type BW25113 and the  $\Delta eldB$  mutant for ten antibiotics.

Antibiotics	MICs value ( $\mu\text{g/mL}$ )	
	BW25113	$\Delta eldB$
Ampicillin	4	4
Polymyxin B	0.5	0.5
Cefoxitin	8	4
Ceftazidime	0.5	<0.25
Imipenem	<0.125	<0.125
Cefotaxime	<0.25	<0.25
Cefepime	<0.5	<0.5
Ciprofloxacin	<0.125	<0.125
Gentamicin	<0.5	<0.5
Tetracycline	2	2

575  
576

577  
578

## FIGURE LEGENDS

- 579 **Figure 1. Conserved C-terminal transmembrane domain in *ElaB*.** Alignment of amino acid  
580 sequences among *ElaB* and other hypothetical membrane proteins from different bacterial  
581 species was performed based on Dense Alignment Surface method  
582 (<http://www.sbc.su.se/~miklos/DAS>). The predicted transmembrane motif is underlined.
- 583 **Figure 2. *ElaB* is an inner membrane anchored protein.** Coexpression of the mCherry fusion  
584 protein *ElaB* or LacZ in BW25113 at a turbidity at 600 nm of 1.0. mCherry fluorescence  
585 (middle panels) is overlaid with the phase contrast images (left panels) in the same field  
586 to get merged images (right panels). Three independent cultures were used and only one  
587 representative figure is shown here.
- 588 **Figure 3. *ElaB* localization using Western blot.** (A) Cell lysates and fractions containing the inner  
589 and outer membrane proteins were obtained as described in the Methods. The His-tag  
590 antibody was used to determine *ElaB* levels when overexpress *elaB* using pCA24N-*elaB*.  
591 Cells producing inner membrane protein MacB and outer membrane protein OmpA were  
592 also used as positive controls. (B) Expression of *ElaB* via pCA24N and chromosomal  
593 *ElaB*-GFP, and its levels in soluble fractions and membrane fractions were determined.  
594 GFP antibody was used to determine *ElaB* levels when coexpressed *gfp* and *elaB* in  
595 chromosome
- 596 **Figure 4. *ElaB* is induced during the stationary phase, and *elaB* is regulated by RpoS.** (A) Cells  
597 grown to the exponential phase (OD<sub>600</sub> 0.7) and stationary phase (OD<sub>600</sub> 6.0) were  
598 harvested, and total RNA was isolated. The transcriptional level of *elaB* was determined  
599 using qRT-PCR and calculated using 2<sup>-ΔΔCt</sup>. The expression of *elaB* was normalized to  
600 that of *rrsG*. The relative expression of *elaB* in the stationary phase was compared to that  
601 in the exponential phase, and the relative expression in M9+Glu medium was normalized  
602 to that in LB medium. (B) *elaB* expression is induced by RpoS. The Δ*rpoS* cells grown to  
603 the exponential phase (OD<sub>600</sub> 0.7) and stationary phase (OD<sub>600</sub> 6.0) were harvested, and  
604 the transcriptional level of *elaB* was determined as in (A). The cells harboring pCA24N-  
605 *rpoS* were induced with 1 mM IPTG for 1 h at OD<sub>600</sub> 1.0, and cells were harvested, and  
606 total RNA was isolated. The expression of *elaB* was determined, and vector pCA24N was  
607 used as a negative control. Three independent cultures for each strain were used in A, B,  
608 and the data are shown as means ± standard deviations. For statistical analysis, *p* < 0.01 is  
609 marked as \*\*. (C) The promoter region of *elaB* and the sequences of the two probes each  
610 containing one putative RpoS binding site. The numbers indicate the locations relative to  
611 the start codon A of *elaB*. Two predicted binding sites of RpoS are marked. The “-10”  
612 and “-35” regions are highlighted in green and light blue. The ribosome binding site  
613 (RBS) is also highlighted in gray. The start codon of *elaB* is shown in red letters. The  
614 black arrows pointed to the mutated sequence of “-10” and “-35” regions in RpoS binding  
615 site 2. (D) Purification of RpoS. A total of 20 μg protein was loaded for each lane. M  
616 indicates protein marker. (E) RpoS binds to Probe 2 in a concentration-dependent manner  
617 with addition of RNA core polymerase (lanes 1-6). The addition of an excess amount of  
618 unlabeled probe reduced the binding of RpoS to the labeled probe in a concentration-  
619 dependent manner (lanes 7-9). (F) RpoS could not bind to Probe 1 (lanes 1-9) or the  
620 mutant RpoS binding site 2 (Probe 3, lanes 10-18) under the same conditions.
- 621 **Figure 5. Promoter activity of *elaB* is induced by RpoS.** (A) Wild-type BW25113 (WT) and  
622 Δ*rpoS* harboring pHGR01-*PelaB* and pHGR01-M*pelaB* in the stationary phases were  
623 collected, and β-galactosidase activities were tested. (B) Δ*rpoS*/pHGR01-*PelaB* and  
624 Δ*rpoS*/pHGR01-M*PelaB* cells expressing RpoS were induced with 0.5 mM IPTG for 2 h  
625 at OD<sub>600</sub> 1.0, and β-galactosidase activities were tested. The pCA24N vector was used as

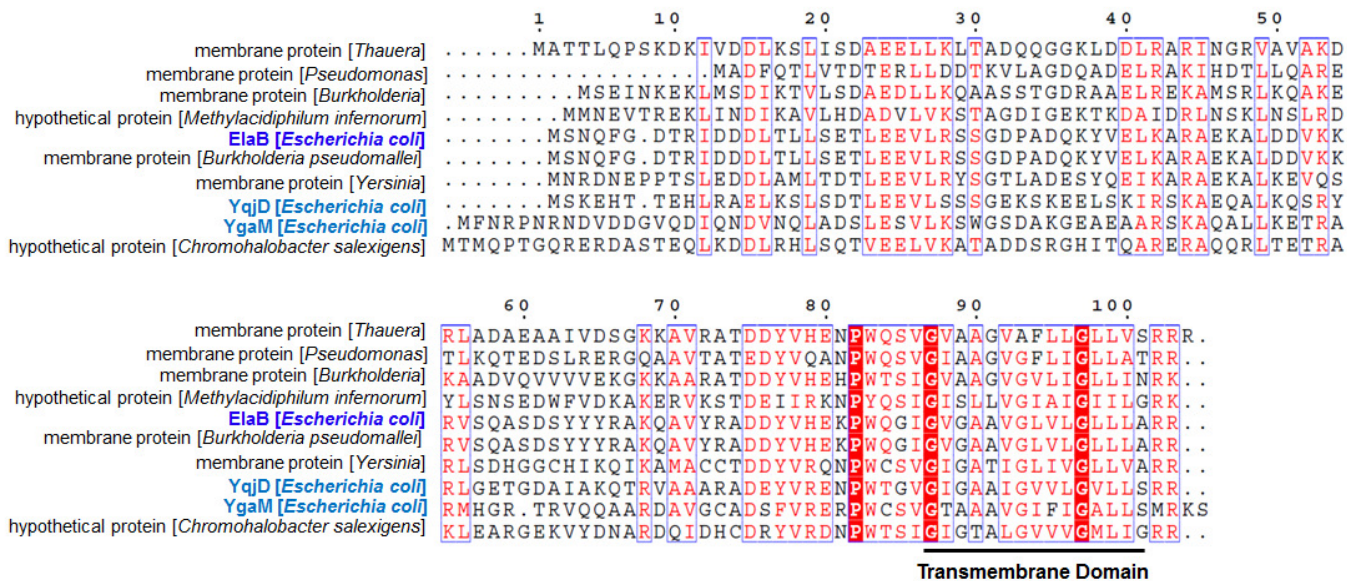
626  
627  
628  
629  
630  
631  
632  
633  
634  
635  
636  
637  
638  
639  
640  
641  
642  
643  
644  
645  
646  
647  
648  
649

a negative control. Three independent cultures for each strain were used. For statistical analysis,  $p < 0.01$  is marked as \*\*.

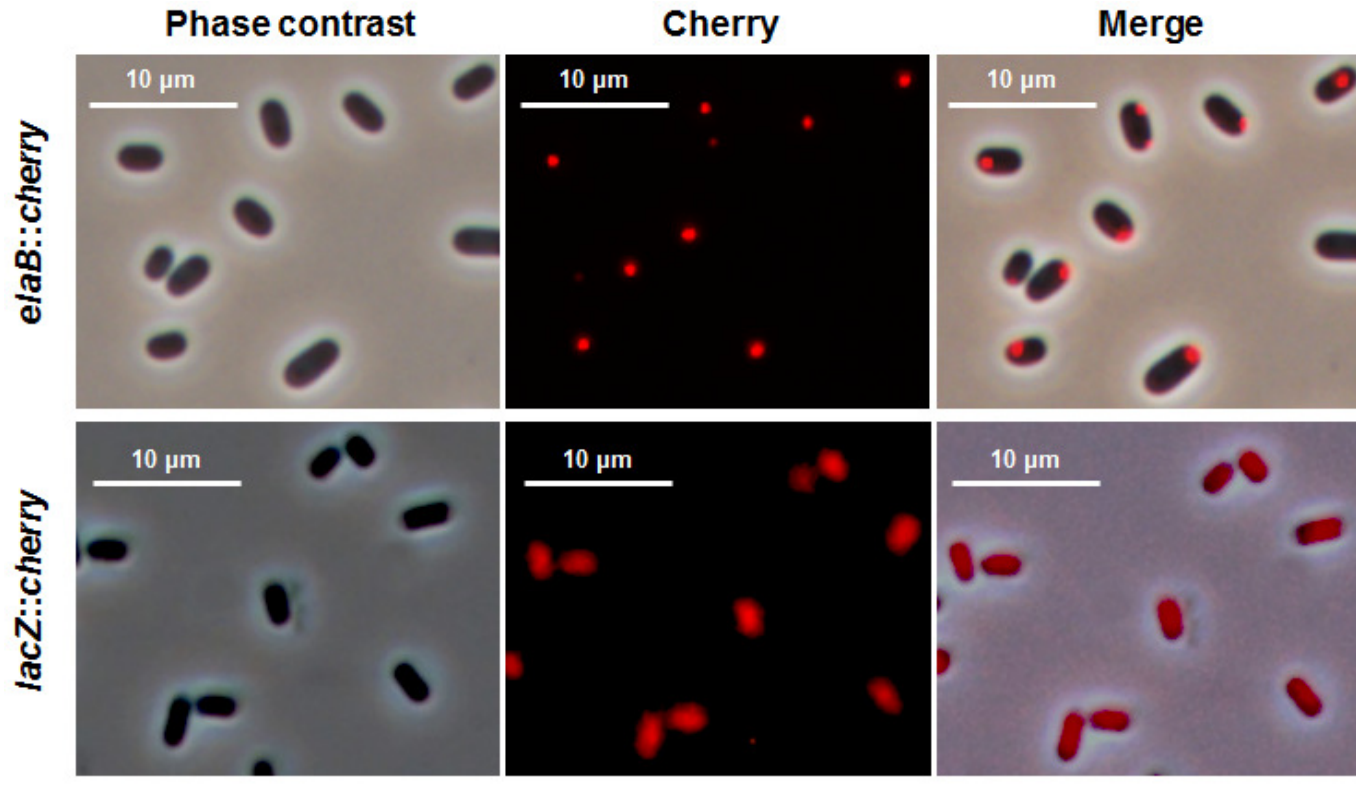
**Figure 6. *ElaB* increases survival during heat and oxidative stress.** (A) Wild-type BW25113 (WT) and  $\Delta elaB$  cells were grown until the turbidity reached 1.0, and were treated with heat stress (65 °C for 5 min and 10 min), then cell survival (%) was tested. (B) Overnight cultures were diluted and until the turbidity reached 0.5, then 1 mM IPTG was added for 2 h. Then OD<sub>600</sub> was adjusted to 1.0, and cell survival was determined as (A). (C) Cells as (A) were treated with 10 mM H<sub>2</sub>O<sub>2</sub> for the indicated times, then cell survival was assayed. (D) Cells were collected as (B) and cell survival was determined after treated with 10 mM H<sub>2</sub>O<sub>2</sub>. Each assay was performed with three independent cultures, and one standard deviation is shown. Significant changes are marked with an asterisk for  $p < 0.05$  and two asterisk for  $p < 0.01$ .

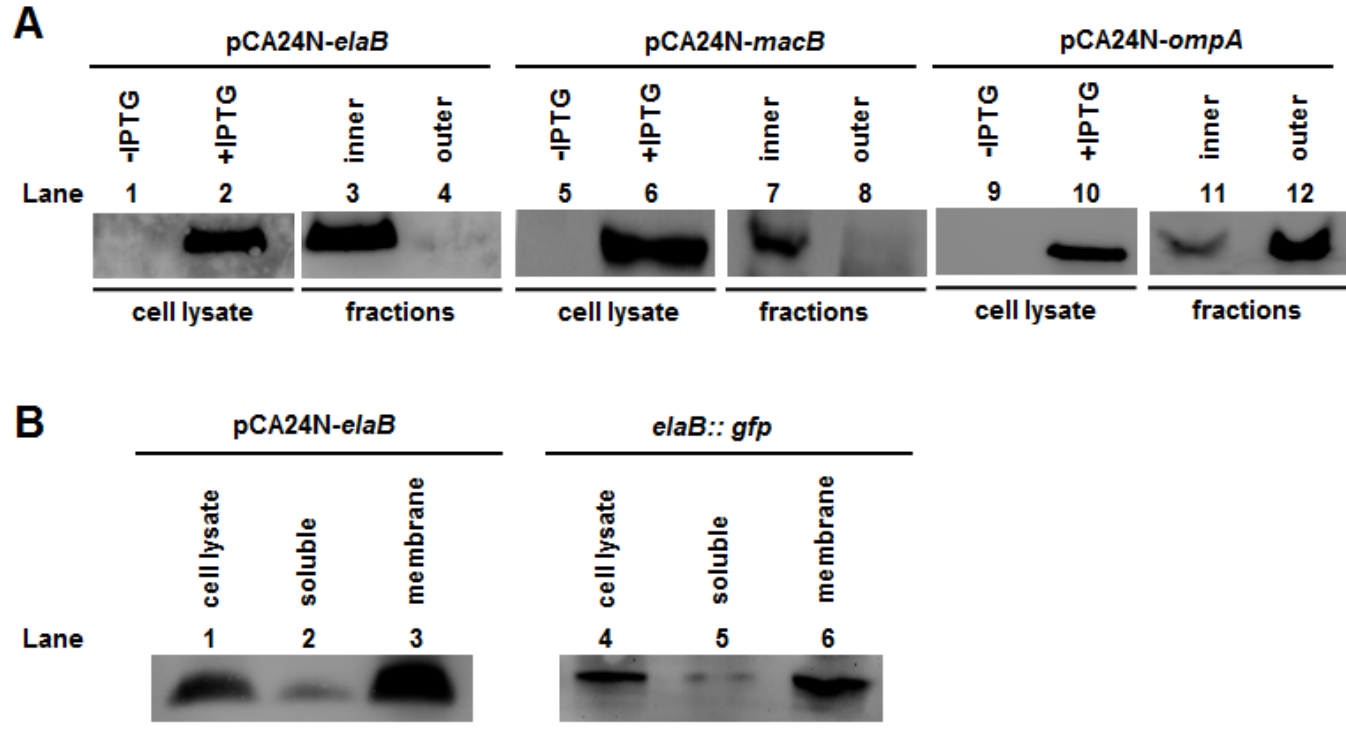
**Figure 7. *ElaB* decreases persistence.** Survival of wild-type BW25113 (WT) and  $\Delta elaB$  cells was determined with 100 µg/mL ampicillin (A) and 5 µg/mL ciprofloxacin at the indicated time points (B). Overnight cultures were diluted and cultured until the turbidity reached 1.0 before adding ampicillin or ciprofloxacin in A and B. Cell survival (CFU/mL) upon expressing *elaB* via pCA24N-*elaB* in the wild-type and  $\Delta elaB$  cells respectively was determined with 100 µg/mL ampicillin (C) and 5 µg/mL ciprofloxacin at the indicated time points (D) Overnight cultures were diluted and cultured until the turbidity reached 0.5, then 1 mM IPTG was added for 2 h. Then, the turbidity was adjusted to 1.0, the cells were treated with antibiotics, and persistence was determined at the indicated time points. Empty plasmid pCA24N was used as a negative control. Three independent cultures of each strain were evaluated in A-D.



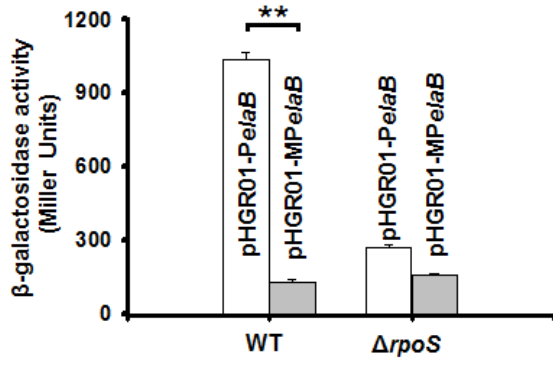


Transmembrane Domain







**A****B**